Photochemical and Electrochemical Properties of Zinc Chlorin−C_{60} Dyad as Compared to Corresponding Free-Base Chlorin−C_{60}, Free-Base Porphyrin−C_{60}, and Zinc Porphyrin−C_{60} Dyads

Shunichi Fukuzumi,*,† Kei Ohkubo,† Hiroshi Imahori,† Jianguo Shao,‡ Zhongping Ou,‡ Gang Zheng,§ Yihui Chen,§ Ravindra K. Pandey,*,§,|| Mamoru Fujitsuka,⊥ Osamu Ito,*,⊥ and Karl M. Kadish*,‡

Contribution from the Department of Material and Life Science, Graduate School of Engineering, Osaka University, CREST, Japan Science and Technology Corporation (JST), 2−1, Yamada-oka, Suita, Osaka 565-0871, Japan, Department of Chemistry, University of Houston, Houston, Texas 77204-5003, Chemistry Division, Photodynamic Therapy Center, Roswell Park Cancer Institute, Buffalo, New York 14263, Department of Nuclear Medicine, Roswell Park Cancer Institute, Buffalo, New York 14263, and Institute of Multidisciplinary Research for Advanced Materials, Tohoku University, CREST, Japan Science and Technology Corporation (JST), Sendai, Miyagi 980-8577, Japan

Received March 1, 2001

Abstract: The photochemical and electrochemical properties of four chlorin−C_{60} or porphyrin−C_{60} dyads having the same short spacer between the macrocycle and the fullerene are examined. In contrast with all the previous results on porphyrin−fullerene dyads, the photoexcitation of a zinc chlorin−C_{60} dyad results in an unusually long-lived radical ion pair which decays via first-order kinetics with a decay rate constant of 9.1×10^3 s^{-1}. This value is 2−6 orders of magnitude smaller than values reported for all other porphyrin or chlorin donor−acceptor of the molecule dyad systems. The formation of radical cations of the donor part and the radical anion of the acceptor part was also confirmed by ESR measurements under photoirradiation at low temperature. The photoexcitation of other dyads (free-base chlorin−C_{60}, zinc porphyrin−C_{60}, and free-base porphyrin−C_{60} dyads) results in formation of the ion pairs which decay quickly to the triplet excited states of the chlorin or porphyrin moiety via the higher lying radical ion pair states as is expected from the redox potentials.

Introduction

Because fullerenes and porphyrins have rich redox properties in both the ground and excited states, they have been utilized as important components for the design of novel artificial photosynthetic systems.[1−8] Fullerenes have a low absorbance in the visible wavelength region, whereas porphyrins generally have strong absorption bands in this region of the spectrum. Thus, most C_{60}-based donor−acceptor systems synthesized to date have utilized porphyrins as an antenna for efficient light capture in the visible region of the spectrum.[1−8] Although natural photosynthesis utilizes chlorophylls as antenna molecules, only a few model compounds have been synthesized where a chlorophyll-like donor (a chlorin) is linked with C_{60},[9−11] and

* To whom correspondence should be addressed. E-mail: fukuzumi@ap.chem.eng.osaka-u.ac.jp, Ravindra.Pandey@RoswellPark.org, ito@tagen.tohoku.ac.jp, and KKadish@uh.edu.

† Osaka University.

‡ University of Houston.

§ Chemistry Division, Photodynamic Therapy Center, Roswell Park Cancer Institute.

|| Department of Nuclear Medicine, Roswell Park Cancer Institute.

⊥ Tohoku University.

(1) (a) Imahori, H.; Sakata, Y. *Adv. Mater.* **1997**, *9*, 537. (b) Imahori, H.; Sakata, Y. *Eur. J. Org. Chem.* **1999**, 2445. (c) Guldi, D. M. *Chem. Commun.* **2000**, 321. (d) Guldi, D. M.; Prato, M. *Acc. Chem. Res.* **2000**, *33*, 695. (e) Fukuzumi, S.; Guldi, D. M. In *Electron Transfer in Chemistry*; Balzani, V., Ed.; Wiley-VCH: Weinheim, 2001; Vol. 2, pp 270−337.

(2) Fukuzumi, S.; Imahori, H. In *Electron Transfer in Chemistry*; Balzani, V., Ed.; Wiley-VCH: Weinheim, 2001; pp 927−975.

(3) Guldi, D. M.; Kamat, P. V. In *Fullerenes, Chemistry, Physics, and Technology*; Kadish, K. M., Ruoff, R. S., Eds.; Wiley-Interscience: New York, 2000; pp 225−281.

(4) (a) Gust, D.; Moore, T. A. In *The Porphyrin Handbook*; Kadish, K. M., Smith, K. M., Guilard, R., Eds.; Academic Press: San Diego, CA, 2000; Vol. 8, pp 153−190. (b) Gust, D.; Moore, T. A.; Moore, A. L. *Res. Chem. Intermed.* **1997**, *23*, 621. (c) Gust, D.; Moore, T. A.; Moore, A. L. *Acc. Chem. Res.* **2001**, *34*, 40.

(5) (a) Martín, N.; Sánchez, L.; Illescas, B.; Pérez, I. *Chem. Rev.* **1998**, *98*, 2527. (b) Diederlich, F.; Gómez-López, M. *Chem. Soc. Rev.* **1999**, *28*, 263.

(6) (a) Jensen, A. W.; Wilson, S. R.; Schuster, D. I. *Bioorg. Med. Chem.* **1996**, *4*, 767. (b) Schuster, D. I.; Cheng, P.; Wilson, S. R.; Prokhorenko, V.; Katterle, M.; Holzwarth, A. R.; Braslavsky, S. E.; Klihm, G.; Williams, R. M.; Luo, C. *J. Am. Chem. Soc.* **1999**, *121*, 11599. (c) Wilson, S. R.; Schuster, D. I.; Nuber, B.; Meier, M. S.; Maggini, M.; Prato, M.; Taylor, R. *Fullerenes*; Kadish, K. M., Ruoff, R. S., Eds.; John Wiley & Sons: New York, 2000; Chapter 3, pp 91−176.

(7) Sun, Y.-P.; Riggs, J. E.; Guo, Z.; Rollins, H. W. In *Optical and Electronic Properties of Fullerenes and Fullerene-Based Materials*; Shinar, J., Vardeny, Z. V., Kafafi, Z. H., Eds.; Marcel Dekker: New York, 2000; pp 43−81.

(8) (a) Bell, T. D. M.; Smith, T. A.; Ghiggino, K. P.; Ranasinghe, M. G.; Shephard, M. J.; Paddon-Row, M. N. *Chem. Phys. Lett.* **1997**, *268*, 223. (b) Guldi, D. M.; Luo, C.; Prato, M.; Dietel, E.; Hirsch, A. *Chem. Commun.* **2000**, 373.

(9) (a) Helaja, J.; Tauber, A. Y.; Abel, Y.; Tkachenko, N. V.; Lemmetyinen, H.; Kilpeläinen, I.; Hynninen, P. H. *J. Chem. Soc., Perkin Trans. 1* **1999**, 2403. (b) Tkachenko, N. V.; Rantala, L.; Tauber, A. Y.; Helaja, J.; Hynninen, P. H.; Lemmetyinen, H. *J. Am. Chem. Soc.* **1999**, *121*, 9378. (c) Tkachenko, N. V.; Vuorimaa, E.; Kesti, T.; Alekseev, A. S.; Tauber, A. Y.; Hynninen, P. H.; Lemmetyinen, H. *J. Phys. Chem. B* **2000**, *104*, 6371.

(10) Zheng, G.; Dougherty, T. J.; Pandey, R. K. *Chem. Commun.* **1999**, 2469.

10.1021/ja015738a CCC: $20.00
Published on Web 10/05/2001

Scheme 1

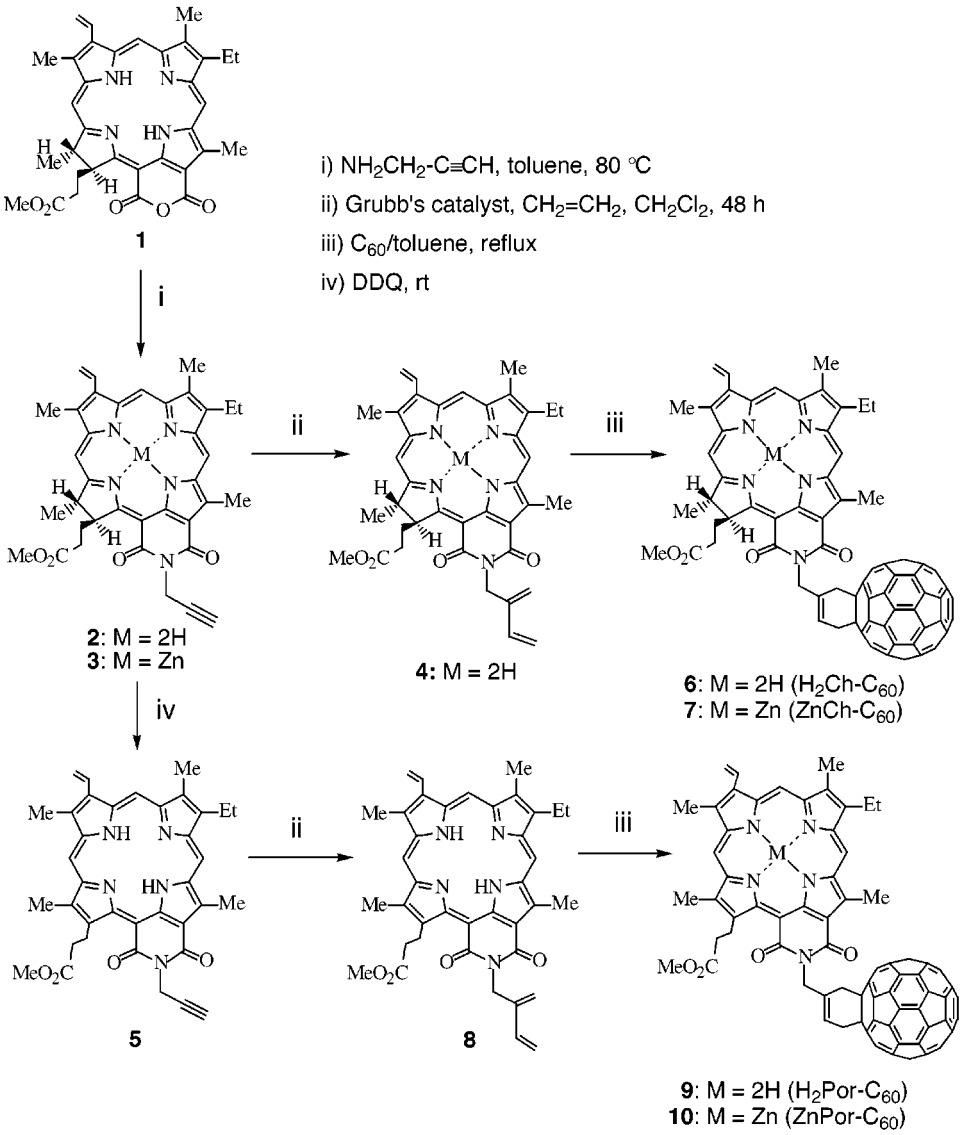

only one of these compounds (a chlorin−C_{60} dyad) has been examined as to its photochemical properties.[9] It is thus of great interest to examine the use of a chlorin as an electron donor instead of a fully conjugated porphyrin in the C_{60}-linked dyad so that comparisons might be made between these related systems. A number of porphyrin−C_{60} dyads have been reported in the literature,[1−8] but the different linkages and geometries between the various porphyrin−C_{60} systems and the single photochemically investigated chlorin-containing dyad have precluded a direct comparison between the redox and photochemical properties of these two systems.

In this study, we have designed and synthesized both chlorin (H_2Ch)−C_{60} and porphyrin (H_2Por)−C_{60} dyads as well as the Zn analogues (ZnCh−C_{60} and ZnPor−C_{60}), all of which have the same linkage so that we might quantitatively extract the results of utilizing a chlorophyll-like donor (a chlorin) instead of a fully conjugated porphyrin. The electrochemical and photochemical properties of these compounds are then studied using cyclic voltammetry and laser flash photolysis, respectively. Unique electrochemical and photochemical properties of ZnCh−C_{60} are revealed in comparison with those of the other dyads.

(11) (a) Kutzki, O.; Walter, A.; Montforts, F.-P. *Helv. Chim. Acta* **2000**, *83*, 2231. (b) Montforts, F.-P.; Kutzki, O. *Angew. Chem., Int. Ed.* **2000**, *39*, 599.

Experimental Section

Materials. Tetramethyl-*p*-benzosemiquinone radical anion in benzonitrile was prepared by proportionation reaction of tetramethyl-*p*-benzoquinone with the dianion obtained by a deprotonation of the corresponding hydroquinone with tetrabutylammonium hydroxide.[12,13] Tris(2,2′-bipyridyl)ruthenium dichloride hexahydrate, $[Ru(bpy)_3]Cl_2 \cdot 6H_2O$, was obtained commercially from Aldrich. The oxidation of $[Ru(bpy)_3]Cl_2$ with lead dioxide in aqueous H_2SO_4 gives $[Ru(bpy)_3]^{3+}$, which is isolated as the PF_6^- salt, $[Ru(bpy)_3](PF_6)_3$.[14] Tetrabutylammonium perchlorate (*n*-Bu_4NClO_4), used as a supporting electrolyte for the electrochemical measurements, obtained from Fluka Fine Chemical, was recrystallized from ethanol and dried in vacuo prior to use. Benzonitrile was purchased from Wako Pure Chemical Ind., Ltd., and purified by successive distillation over P_2O_5.[15]

The synthesis and characterization of H_2Ch−C_{60}, H_2Po−C_{60}, the Zn analogues (ZnCh−C_{60} and ZnPor−C_{60}), and the reference compounds have been performed according to Scheme 1. For synthesis of the corresponding porphyrin−fullerene analogues, the purpurin-18-*N*-propargylimide (synthesis is described in Supporting Information, S1)

(12) Fukuzumi, S.; Yorisue, T. *Bull. Chem. Soc. Jpn.* **1992**, *65*, 715.
(13) Fukuzumi, S.; Nakanishi, I.; Suenobu, T.; Kadish, K. M. *J. Am. Chem. Soc.* **1999**, *121*, 3468.
(14) DeSimone, R. E.; Drago, R. S. *J. Am. Chem. Soc.* **1970**, *92*, 2343.
(15) Perrin, D. D.; Armarego, W. L. F. *Purification of Laboratory Chemicals*; Butterworth-Heinemann: Oxford, 1988.

was converted into the related porphyrin, also known as "emeraldin", by DDQ (2,3-dichloro-5,6-dicyano-*p*-benzoquinone) treatment.[16]

Chlorin-diene 4. Propargylimide **2** (85 mg, 0.14 mmol) was dissolved in 10 mL of dichloromethane (CH_2Cl_2), followed by 12 mg of Grubbs' catalyst (10 mol %). The synthesis of **2** is described in Supporting Information (S1). The reaction mixture was stirred under ethylene gas at room temperature for 48 h. After removing solvent and excess ethylene, the mixture was chromatographed on a silica plate with 1% acetone/CH_2Cl_2 as the mobile phase. The fast moving band was identified as desired diene **4** with a 40% conversion yield (36 mg). The slow moving band was identified as the starting material. There was no byproduct formation in this reaction. Melting point: 185 °C. FAB MS (*m*/*z*): 644.6 (M + 1) and 643.6 (M). Anal. Calcd for $C_{39}H_{41}N_5O_4\cdot(^1/_2)H_2O$: C, 71.74; H, 6.49; N, 10.73. Found: C, 72.11; H, 6.39; N, 10.70. UV−vis (CH_2Cl_2, nm (ϵ)): 365 (4.7×10^4), 416 (1.3×10^5), 512 (6.5×10^3), 548 (2.3×10^4), 647 (7.7×10^3), 707 (4.8×10^4). ^{1}H NMR (400 MHz, 5.0 mg/mL $CDCl_3$, δ ppm): 9.51, 9.26 and 8.57 (each s, 1H, 5-H, 10-H and 20-H), 7.84 (dd, $J = 18$ Hz, 12 Hz, 1H, 31-H), 6.70 (dd, $J = 18$ Hz, 12 Hz, 1H, diene-H), 6.25 (d, $J = 18$ Hz, 1H, 32-H), 6.12 (d, $J = 12$ Hz, 1H, 32-H), 5.64 (d, $J = 18$ Hz, 1H, diene-H), 5.41 (m, 1H, 17-H), 5.33 (d, 1H, diene-H), 5.31 (s, 2H, N−CH_2), 5.21 (d, $J = 17$ Hz, 2H, diene-H), 4.36 (q, $J = 7$ Hz, 1H, 18-H), 3.78, 3.56, 3.33 and 3.08 (each s, 3H, CH_3), 3.54 (q, $J = 8$ Hz, 2H, 8-*CH*$_2$CH$_3$), 2.71, 2.41 and 2.00 (each m, total 4H, 171-CH_2 and 172-CH_2), 1.79 (d, $J = 7$ Hz, 3H, 18-CH_3), 1.63 (t, $J = 8$ Hz, 3H, 8-CH$_2$*CH*$_3$), −0.03 and −0.15 (each br s, 1H, *N*-H).

Porphyrin-*N*-propargylimide Methyl Ester 5. Purpurin 18-*N*-propargylimide, **2**, (820 mg, 1.27 mmol) was dissolved in 100 mL of dry CH_2Cl_2 and stirred under argon. A solution of 2,3-dichloro-5,6-dicyano-*p*-benzoquinone (DDQ) (530 mg in 10 mL methanol) was added in portions over 30 min. The reaction mixture was left stirring for another 30 min before pouring into water. After washing with 6 × 800 mL of water to remove the excess DDQ, the crude product was further washed with hexanes to remove most of the chlorins ($\lambda_{max} =$ 705 nm). Finally, after purification by column chromatography with 2% MeOH/CH_2Cl_2, the desired porphyrin was obtained in 55% yield (428 mg). HRMS for $C_{37}H_{35}N_5O_4$: calcd, 614.2683 (M + 1); found, 614.2. ^{1}H NMR (400 MHz, 5.0 mg/mL $CDCl_3$, δ ppm): 8.99, 8.89 and 8.88 (each s, 1H, 5-H, 10-H and 20-H), 7.67 (dd, $J = 18$ Hz, 12 Hz, 1H, 31-H), 6.06 (d, $J = 18$ Hz, 1H, 32-H), 6.03 (d, $J = 12$ Hz, 1H, 32-H), 5.34 (d, 2H, $J = 2$ Hz, *N*-CH_2), 4.05 (t, $J = 8$ Hz, 2H, 17-*CH*$_2$CH$_2$CO$_2$CH$_3$), 3.64, 3.63, 3.20, 3.17 and 3.13 (each s, 3H, 2-, 7-, 12-, 18-CH_3 and CO_2CH_3), 3.61 (q, $J = 8$ Hz, 2H, 8-*CH*$_2$CH$_3$), 3.15 (t, 2H, 17-CH$_2$*CH*$_2$CO$_2$CH$_3$), 2.46 (t, $J = 2$ Hz, 1H, CCH), 1.56 (t, $J = 8$ Hz, 3H, 8-CH$_2$*CH*$_3$), 10.16 and 9.87 (each br s, 1H, 2 × *N*-H).

Chlorin−C_{60} Dyad 6. Diene **4** (30 mg, 0.047 mmol) and C_{60} (44 mg, 0.061 mmol) were mixed in 20 mL toluene and refluxed for 2 h. After removing the solvent, the crude product was chromatographed on silica plate with 1% methanol/CH_2Cl_2, and two bands were collected. Desired dyad **6** was obtained in 30% yield (19 mg) from the fast moving band, and the starting diene **4** was recovered in 50% yield (14 mg) from the slow moving band. Melting point: 197 °C. HRMS for $C_{99}H_{41}N_5O_4$: calcd, 1364.3270 (M + 1); found, 1364.3273. UV−vis (CH_2Cl_2, nm (ϵ)): 365 (4.8×10^4), 419 (1.0×10^5), 512 (6.4×10^3), 551 (1.9×10^4), 653 (7.1×10^3), 710 (3.7×10^4). ^{1}H NMR (400 MHz, 5.0 mg/mL $CDCl_3$, δ ppm): 9.48, 9.30 and 8.49 (each s, 1H, 5-H, 10-H and 20-H), 7.85 (dd, $J = 18$ Hz, 12 Hz, 1H, 31-H), 7.22 (t, $J = 5$ Hz, 1H, cyclohexene-H), 6.26 (d, $J = 18$ Hz, 1H, 32-H), 6.14 (d, $J = 12$ Hz, 1H, 32-H), 5.67 (ABX, 2H, *N*-CH_2), 5.29 (m, 1H, 17-H), 4.33 (ABX, 2H, cyclohexene-H), 4.29 (q, $J = 7$ Hz, 1H, 18-H), 3.98 (d, $J = 6$ Hz, 2H, cyclohexene-H), 3.75, 3.53, 3.30 and 3.12 (each s, 3H, CH_3), 3.59 (q, $J = 8$ Hz, 2H, 8-*CH*$_2$CH$_3$), 2.69, 2.41 and 1.88 (each m, total 4H, 171-CH_2 and 172-CH_2), 1.63 (d, $J = 7$ Hz, 3H, 18-CH_3), 1.61 (t, $J = 8$ Hz, 3H, 8-CH$_2$*CH*$_3$), −0.05 (br s, 2H, 2 × *N*-H).

Chlorin−C_{60} Dyad (Zn Complex) 7. Chlorin−C_{60} dyad **6** (7.5 mg, 0.0055 mmol) was dissolved in 20 mL of CH_2Cl_2, followed by 5 mL of saturated $Zn(OAc)_2$ in methanol. The reaction mixture was refluxed for 1h. After regular workup, the crude product was chromatographed on a silica plate with 3% methanol/CH_2Cl_2. The title compound was obtained in 6.0 mg yield (75% yield). Melting point: 154 °C. FAB MS (*m*/*z*): 1427.9 (M + 1), 720.7 (C_{60}). UV−vis (CH_2Cl_2, nm (ϵ)): 404 (5.6×10^4), 425 (8.6×10^4), 515 (5.1×10^3), 557 (7.9×10^3), 632 (1.0×10^4), 683 (4.0×10^4). ^{1}H NMR (400 MHz, 5.0 mg/mL $CDCl_3$, δ ppm): 9.26, 9.14 and 8.28 (each s, 1H, 5-H, 10-H and 20-H), 7.82 (dd, $J = 18$ Hz, 12 Hz, 1H, 31-H), 7.13 (t, $J = 5$ Hz, 1H, cyclohexene-H), 6.10 (d, $J = 18$ Hz, 1H, 32-H), 6.01 (d, $J = 12$ Hz, 1H, 32-H), 5.42 (ABX, 2H, N−CH_2), 5.26 (m, 1H, 17-H), 4.28 (ABX, 2H, cyclohexene-H), 4.13 (q, $J = 7$ Hz, 1H, 18-H), 4.00 (d, $J = 6$ Hz, 2H, cyclohexene-H), 3.58 (q, $J = 8$ Hz, 2H, 8-*CH*$_2$CH$_3$), 3.49, 3.34, 3.20 and 3.12 (each s, 3H, 4 × CH_3), 2.56, 2.26 and 1.85 (each m, total 4H, 171-CH_2 and 172-CH_2), 1.61 (t, $J = 8$ Hz, 3H, 8-CH$_2$*CH*$_3$), 1.58 (d, $J = 7$ Hz, 3H, 18-CH_3).

Preparation of Porphyrin-Diene 8. A mixture of propargylimide **5** (400 mg, 0.65 mmol) and Grubbs' catalyst (55 mg, 10 mol %) was dissolved in 50 mL of CH_2Cl_2. The reaction mixture was stirred under ethylene gas at room temperature for 64 h. After removing the solvent, the crude product was separated by silica column chromatography with 2.5% MeOH/CH_2Cl_2, and the resulting product was further purified by silica plate with 2% MeOH/CH_2Cl_2 to afford the porphyrin-diene in 30% yield (125 mg). EI for $C_{39}H_{39}N_5O_4$: calcd, 642.2996 (M + 1); found, 642.3. ^{1}H NMR (400 MHz, 5.0 mg/mL $CDCl_3$, δ ppm): 9.22, 9.14 and 9.13 (each s, 1H, 5-H, 10-H and 20-H), 7.73 (dd, $J = 18$ Hz, 12 Hz, 1H, 31-H), 6.72 (dd, $J = 18$ Hz, 12 Hz, 1H, diene-H), 6.07 (d, $J = 18$ Hz, 1H, *trans*-32-H), 6.04 (d, $J = 12$ Hz, 1H, *cis*-32-H), 5.79 (d, $J = 18$ Hz, 1H, diene-H), 5.39−5.33 (m, total 5H, 3 × diene-H and *N*-CH_2), 4.02 (t, $J = 8$ Hz, 2H, 17-*CH*$_2$CH$_2$CO$_2$CH$_3$), 3.69, 3.64, 3.29, 3.22 and 3.19 (each s, 3H, 2-, 7-, 12-, 18-CH_3, and CO_2CH_3), 3.67 (q, $J = 8$ Hz, 2H, 8-*CH*$_2$CH$_3$), 3.14 (t, $J = 8$ Hz, 2H, 17-CH$_2$*CH*$_2$-CO$_2$CH$_3$), 1.62 (t, $J = 8$ Hz, 3H, 8-CH$_2$*CH*$_3$), 10.85 and 10.62 (each br s, 1H, 2 × *N*-H).

Porphyrin−C_{60} Dyad 9. Diene **8** (55 mg, 0.086 mmol) and C_{60} (65 mg, 0.090 mmol) were mixed in 20 mL of toluene and refluxed for 3 h. After removing the solvent, the residue was chromatographed on a silica plate with 1% methanol/CH_2Cl_2. Desired dyad **9** was obtained in 10% (12 mg) yield. UV−vis (benzene, nm (ϵ)): 438 (1.1×10^5), 617 (1.0×10^4), 669 (1.3×10^4). HRMS for $C_{99}H_{39}N_5O_4$: calcd, 1362.2996 (M + 1); found, 1362.3. ^{1}H NMR (400 MHz, 5.0 mg/mL $CDCl_3$, δ ppm): 4.33 (m, 2H, cyclohexene-H), 4.29 (q, $J = 7$ Hz, 1H, 18-H), 3.98 (d, $J = 6$ Hz, 2H, cyclohexene-H), 3.75, 3.53, 3.30 and 3.12 (each s, 3H, CH_3), 3.59 (q, $J = 8$ Hz, 2H, 81-CH_2), 2.69, 2.41 and 1.88 (each m, total 4H, 171-CH_2 and 172-CH_2), 1.63 (d, $J = 7$ Hz, 3H, 18-CH_3), 1.61 (t, $J = 8$ Hz, 3H, 82-CH_3), −0.05 (br s, 2H, 2 × N−H), 9.81, 9.77 and 9.74 (each s, 1H, 5-H, 10-H and 20-H), 8.01 (dd, $J = 18$ Hz, 12 Hz, 1H, 31-H), 7.34 (t, $J = 6$ Hz, 1H, 1 × cyclohexene-H), 6.21 (d, $J = 18$ Hz, 1H, *trans*-32-H), 6.11 (d, $J = 12$ Hz, 1H, *cis*-32-H), 5.70 (s, 2H, *N*-CH_2), 4.40 (s, 2H, 2 × cyclohexene-H), 4.23 (t, $J = 8$ Hz, 2H, 17-*CH*$_2$CH$_2$CO$_2$CH$_3$), 4.07 (d, $J = 6$ Hz, 2H, 2 × cyclohexene-H), 3.93 (q, $J = 8$ Hz, 2H, 8-*CH*$_2$CH$_3$), 3.83, 3.73, 3.49, 3.482 and 3.479 (each s, 3H, 2-, 7-, 12-, 18-CH_3 and CO_2CH_3), 3.39 (t, $J = 8$ Hz, 2H, 17-CH$_2$*CH*$_2$CO$_2$CH$_3$), 1.76 (t, $J = 8$ Hz, 3H, 8-CH$_2$*CH*$_3$), 12.43 (br s, 2H, 2 × *N*-H).

Porphyrin−C_{60} Dyad (Zn Complex) 10. Dyad **9** (15 mg, 0.011 mmol) was refluxed in 40 mL of CH_2Cl_2 with 10 mL of saturated $Zn(OAc)_2$ in methanol for 1 h. After the standard workup, the crude product was recrystallized from CH_2Cl_2/hexanes to give 11.0 mg of the title compound (70% yield). UV−vis (benzene, nm (ϵ)): 331 (4.6×10^4), 446 (8.9×10^4), 664 (1.6×10^4).

Electrochemical Measurements. Cyclic voltammetry (CV) measurements were performed on an EG&G model 173 potentiostat coupled with an EG&G model 175 universal programmer in deaerated benzonitrile solution containing 0.10 M *n*-Bu_4NClO_4 as a supporting electrolyte at 298 K. A three-electrode system was used and consisted of a glassy carbon working electrode, a platinum wire counter electrode, and a saturated calomel reference electrode (SCE). The reference electrode was separated from the bulk solution by a fritted-glass bridge filled with the solvent/supporting electrolyte mixture. Thin-layer spectroelectrochemical measurements were carried out at an optically

(16) Kozyrev, A. N.; Zheng, G.; Lazarou, E.; Dougherty, T. J.; Smith, K. M.; Pandey, R. K. *Tetrahedron Lett.* **1997**, *38*, 3335.

transparent platinum thin-layer working electrode using a Hewlett-Packard model 8453 diode array spectrophotometer coupled with an EG&G model 173 universal programmer.

Spectral Measurements. Absorption spectra were recorded on a Shimadzu UV-3100 PC UV−vis NIR spectrophotometer. Fluorescence spectra were recorded on a Spex Fluorolog F112X spectrofluorometer. The fluorescence quantum yield was determined by the relative method using optically dilute solutions of 3,3′-diethyloxatricarbocyanine iodide in ethanol ($\Phi = 0.49$) as reference. Time-resolved fluorescence spectra were measured by a single-photon counting method using second harmonic generation (SHG, 410 nm) of a Ti:sapphire laser (Spectra-Physics, Tsunami 3950-L2S, 1.5 ps fwhm) and a streakscope (Hamamatsu Photonics, C4334−01) equipped with a polychromator (Acton Research, SpectraPro 150) as an excitation source and a detector, respectively. Nanosecond transient absorption measurements were carried out using a Nd:YAG laser (Spectra-Physics, Quanta-Ray GCR-130, fwhm 6 ns or Continuum, SLII-10, 4−6 ns fwhm) at 355 nm with the power at 30 mJ as an excitation source. For transient absorption spectra in the near-IR region (600−1200 nm), monitoring light from a pulsed Xe-lamp was detected with a Ge-avalanche photodiode (Hamamatsu Photonics, B2834). Photoinduced events in micro- and millisecond time regions were estimated by using a continuous Xe-lamp (150 W) and an InGaAs-PIN photodiode (Hamamatsu Photonics, G5125−10; 600−1200 nm and Hamamatsu 2949; 400−600 nm) as a probe light and a detector, respectively. The output from the photodiodes and a photomultiplier tube was recorded with a digitizing oscilloscope (Tektronix, TDS3032, 300 MHz).

ESR Measurements. A quartz ESR tube (internal diameter: 4.5 mm) containing a deaerated PhCN solution of ZnCh−C_{60} (1.0×10^{-3} M) was irradiated in the cavity of the ESR spectrometer with the focused light of a 1000-W high-pressure Hg lamp (Ushio-USH1005D) through an aqueous filter at low temperature. The ESR spectra in frozen PhCN were measured under nonsaturating microwave power conditions with a JEOL X-band spectrometer (JES-RE1XE) using an attached variable temperature apparatus. The magnitude of modulation was chosen to optimize the resolution and the signal-to-noise (S/N) ratio of the observed spectra when the maximum slope line width (ΔH_{msl}) of the ESR signals was unchanged with larger modulation. The *g* values were calibrated with a Mn^{2+} marker.

Theoretical Calculations. Theoretical calculations were performed on a COMPAQ DS20E computer. The PM3 Hamiltonian was used for the semiempirical MO calculations.[17] Final geometries and energetics were obtained by optimizing the total molecular energy with respect to all structural variables. The heats of formation (ΔH_f) were calculated with the restricted Hartree−Fock (RHF) formalism.

Results and Discussion

ZnCh−C_{60} (**7**), ZnPor−C_{60} dyads (**10**), and their corresponding free-base dyads (**6**: H_2Ch−C_{60}, **9**: H_2Por−C_{60}) were synthesized via a Diels−Alder reaction of the chlorin (**4**) and porphyrin (**8**) with the fullerene as shown in Scheme 1 (see Experimental Section).[10,11] These tetrapyrrolic compounds contain a six-membered fused imide ring system and present an opportunity to design fullerene conjugates containing a spacer with a defined length and geometry. The ^{1}H NMR spectra of the dyads revealed the presence of only a single species in solution.[10]

The absorption spectra of **6**, **7**, **9**, and **10** in benzonitrile (PhCN) are reasonable superpositions of the spectra of the component chromophores making up these molecules. Thus, there is no significant electronic interaction between the individual chromophores in their ground-state configuration.

The cyclic voltammograms of ZnCh−C_{60} (**7**) and H_2Ch−C_{60} (**6**) are shown in Figure 1 together with those of unlinked ZnCh (**3**) and H_2Ch (**2**) without C_{60}. The comparison with the unlinked compounds reveals that the cyclic voltammograms of

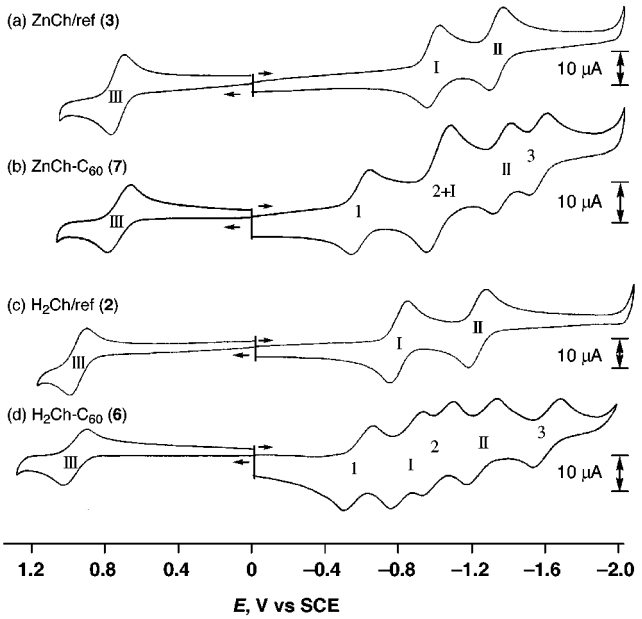

Figure 1. Cyclic voltammograms of (a) **3**, (b) **7**, (c) **2**, and (d) **6** in the presence of 0.10 M *n*-Bu_4NClO_4 in PhCN (processes 1−3 represent reduction of C_{60}, while I and II represent reduction of the macrocycle and III represents oxidation of the macrocycle).

7 and **6** consist of three one-electron reduction processes of C_{60}, two one-electron reduction processes of the macrocyclic ring, and the one-electron oxidation process of the macrocyclic ring. The redox couple of ZnCh/ZnCh$^{\bullet-}$ (**I**) in **7** is overlapped with the redox couple of $C_{60}^{\bullet-}/C_{60}^{2-}$ (**2**) in Figure 1b.[18] Similarly, the one-electron redox potentials of ZnPor−C_{60} (**10**) and H_2Por−C_{60} (**9**) were determined from the cyclic voltammograms. The first one-electron oxidation potentials of the macrocyclic ring ($E°_{ox}$) of **2**, **3**, **6**, **7**, **9**, and **10**, the first one-electron reduction potentials of C_{60} ($E°_{red}$) in the dyads (**6**, **7**, **9**, and **10**), and the first one-electron reduction potentials of the macrocyclic ring of **2** and **3** are listed in Table 1. The $E°_{red}$ values for reduction of linked C_{60} which are attributed to the fullerene moiety are almost invariant, irrespective of the type of linked macrocyclic ring, whereas the $E°_{ox}$ values for oxidation of the macrocycle are shifted in a negative direction in the following order: H_2Por > H_2Ch > ZnPor > ZnCh. Thus, the free energy change of electron transfer from ZnCh to C_{60} in **7**, obtained from the difference between $E°_{ox}$ and $E°_{red}$, is the smallest among the examined dyads.[19]

A deoxygenated PhCN solution containing ZnCh−C_{60} (**7**) gives rise upon a 355 nm laser pulse to a transient absorption spectrum with maxima at 790 and 1000 nm, as shown in Figure 2a (see Supporting Information (S2) for the transient absorption spectrum between 400 and 800 nm). The absorption band at 1000 nm is a clear attribute of the fullerene radical anion, because the one-electron reduction of **7** by tetramethyl-*p*-benzosemiquinone radical anion yields ZnCh−$C_{60}^{\bullet-}$ which exhibits the absorption band at 1000 nm ($\epsilon = 7.0 \times 10^3$ M^{-1} cm^{-1}), as shown in Figure 3.[20] The near-IR band at 1000 nm is known as a diagnostic marker of the monofunctionalized fullerene radical anion.[21−23] The electrochemical oxidation of **7** in PhCN containing 0.2 M *n*-Bu_4NClO_4 at an applied potential

(17) Stewart, J. J. P. *J. Comput. Chem.* **1989**, *10*, 209, 221.

(18) Dubois, D.; Moninot, G.; Kutner, W.; Jones, M. T.; Kadish, K. M. *J. Phys. Chem.* **1992**, *96*, 7137.

(19) The Coulombic term in a polar solvent (PhCN) is assumed to be negligible.

(20) The ϵ value was determined by the titration of ZnCh−C_{60} with tetramethyl-*p*-benzosemiquinone radical anion.[12]

Table 1. One-Electron Oxidation Potentials (E°_{ox}), Reduction Potentials (E°_{red}), Free Energy Chenge of Photoinduced Electron Transfer (ΔG°_{ET}), Electron Transfer Rate Constants (k_{ET}), Free Energy Change of Back Electron Transfer (ΔG°_{BET}), Back Electron Transfer Rate Constants (k_{BET}), and Triplet Decay Rate Constants (k_T) in Deaerated PhCN at 298 K

compound	E°_{ox} V vs SCE	E°_{red} V vs SCE	ΔG°_{ET}, eV	k_{ET} (k_{calc})[a], s^{-1}	ΔG°_{BET}, eV	k_{BET} (k_{calc})[a], s^{-1}	k_T s^{-1}
7 (ZnCh−C_{60})	0.73	−0.60	−0.47	2.4×10^{10} (1.7×10^{10})	−1.33	9.1×10^3 (9.6×10^3)	
10 (ZnPor−C_{60})	0.93	−0.58	−0.33	7.4×10^9 (9.3×10^9)	−1.51		2.0×10^4
6 (H_2Ch−C_{60})	1.00	−0.57	−0.17	4.2×10^9 (2.4×10^9)	−1.57		1.5×10^4
9 (H_2Por−C_{60})	1.15	−0.57	−0.12	6.6×10^8 (1.0×10^9)	−1.72		4.6×10^4
3 (ZnCh/ref)	0.75	−1.00					5.6×10^3
2 (H_2Ch/ref)	0.99	−0.79					6.9×10^3

[a] Calculated based on eq 1.

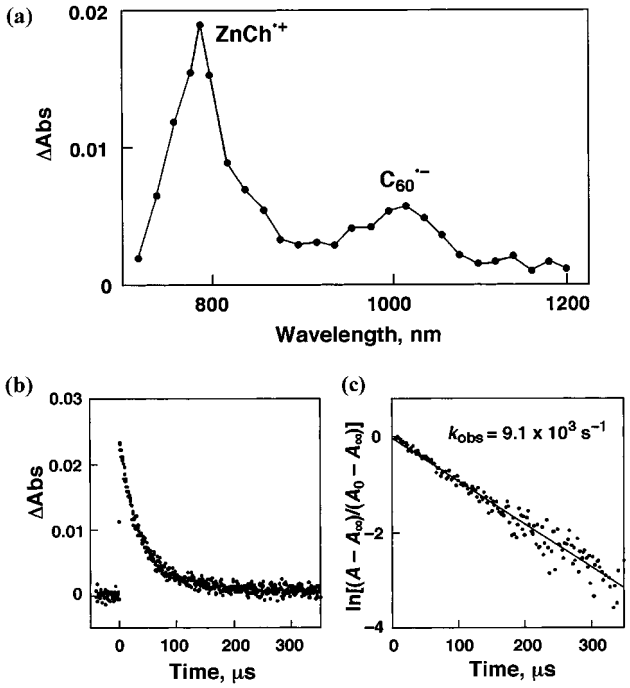

Figure 2. (a) Transient absorption spectrum of ZnCh−C_{60} (**7**) (1.0×10^{-4} M) in deaerated PhCN at 298 K taken at 0.1 μs after laser excitation at 355 nm, (b) the decay profile at 790 nm, and (c) the first-order plot.

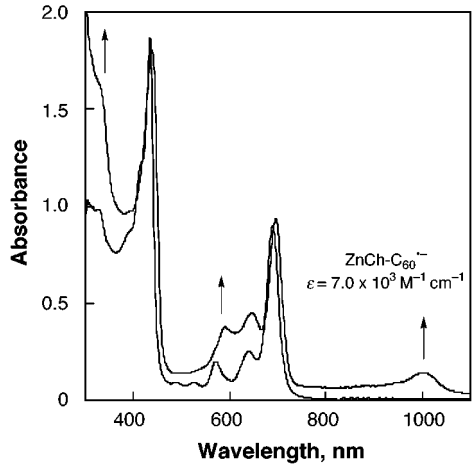

Figure 3. UV−vis spectra of dyad ZnCh−C_{60} (**7**) (1.9×10^{-5} M) and reduced **7** (ZnCh−$C_{60}^{\bullet-}$) produced by the reduction of **7** with tetramethyl-*p*-benzosemiquinone radical anion (2.0×10^{-5} M) in deaerated PhCN at 298 K.

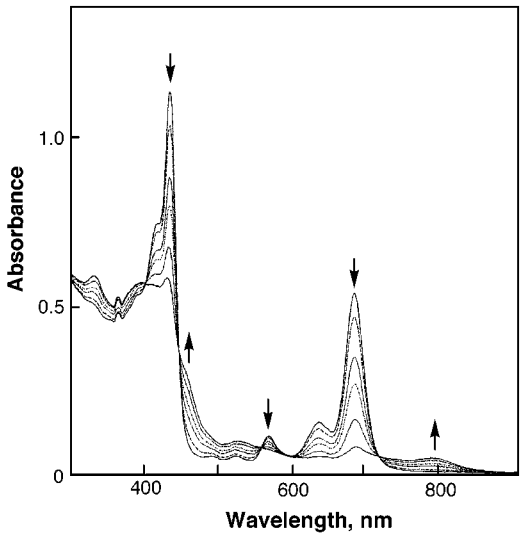

Figure 4. UV−vis spectra of ZnCh−C_{60} (**7**) (2.4×10^{-4} M) during electrochemical oxidation at an applied potential of 0.90 V (vs SCE) in deaerated PhCN at 298 K.

positive of the first reversible oxidation (0.90 V) gives the chlorin π-cation radical (ZnCh$^{\bullet+}$−C_{60}) whose spectrum is shown in Figure 4. This spectrum is almost identical to the transient spectrum in Figure 2a, indicating that the absorption band at 790 nm in the photochemical experiment can be attributed to the radical cation of the chlorin moiety.

The reference chlorin compound, **3**, shows a fluorescence band at 700 nm with a quantum yield of $\Phi = 0.10$, whereas the fluorescence emission is almost quenched for ZnCh−C_{60} (**7**) in PhCN ($\Phi = 0.002$). Next, we measured the fluorescence lifetimes (τ) of **7** and **3** with a time correlated single-photon-counting apparatus by using a 410 nm excitation where the ZnCh moiety is mainly excited. The fluorescence decay curve of **3** monitored at $\lambda = 700$ nm was fitted by a single-exponential decay component. The fluorescence lifetime of **3** (τ(**3**) = 2.6 ns) is significantly reduced when **3** is replaced by **7** (τ(**7**) = 41 ps). The rate constant of electron transfer (k_{ET}) from ^{1}ZnCh* to C_{60} is determined from the difference between τ(**7**)$^{-1}$ and τ(**3**)$^{-1}$ to be 2.4×10^{10} s^{-1} (Table 1). The free energy change of photoinduced electron transfer (ΔG°_{ET}) from the singlet excited state of the ZnCh moiety to the C_{60} moiety in PhCN is determined to be −0.47 eV from the one-electron oxidation potential and the excitation energy (S_1=1.80 eV) of the ZnCh

(21) (a) Fukuzumi, S.; Suenobu, T.; Patz, M.; Hirasaka, T.; Itoh, S.; Fujitsuka, M.; Ito, O. *J. Am. Chem. Soc.* **1998**, *120*, 8060. (b) Fukuzumi, S.; Suenobu, T.; Hirasaka, T.; Sakurada, N.; Arakawa, R.; Fujitsuka, M.; Ito, O. *J. Phys. Chem. A* **1999**, *103*, 5935.

(22) (a) Luo, C.; Guldi, D. M.; Imahori, H.; Tamaki, K.; Sakata, Y. *J. Am. Chem. Soc.* **2000**, *122*, 6535. (b) Imahori, H.; El-Khouly, M. E.; Fujitsuka, M.; Ito, O.; Sakata, Y.; Fukuzumi, S. *J. Phys. Chem. A* **2001**, *105*, 325.

(23) (a) Kadish, K. M.; Gao, X.; Van Caemelbecke, E.; Suenobu, T.; Fukuzumi, S. *J. Phys. Chem. A* **2000**, *104*, 3878. (b) Guldi, D. M.; Asmus, K.-D. *J. Phys. Chem. A* **1997**, *101*, 1472. (c) Guldi, D. M.; Hungerbühler, H.; Asmus, K.-D. *J. Phys. Chem.* **1995**, *99*, 9380.

moiety and the one-electron reduction potential of the C_{60} moiety in **7** (Table 1).[24]

The radical ion pair state ($ZnCh^{\bullet+}-C_{60}^{\bullet-}$) is lower in energy (1.33 eV) than both the triplet excited state of C_{60} (1.45 eV)[25] and ZnCh (1.36−1.45 eV).[26] Thus, photoinduced electron transfer (PET) from the singlet excited state of ZnCh (^{1}ZnCh*) to the C_{60} part of the molecule occurs to produce the radical ion pair, $ZnCh^{\bullet+}-C_{60}^{\bullet-}$, in competition with the intersystem crossing to ^{3}ZnCh* and energy transfer to produce ZnCh−$^1C_{60}$* and ZnCh−$^3C_{60}$*. Electron transfer from ^{3}ZnCh* to C_{60}, as well as electron transfer from ZnCh to $^1C_{60}$* and $^3C_{60}$*, also results in formation of $ZnCh^{\bullet+}-C_{60}^{\bullet-}$. Thus, in any case, the radical ion pair, $ZnCh^{\bullet+}-C_{60}^{\bullet-}$, is formed. The radical ion pair detected in Figure 2 decays via back electron transfer (BET) to the ground-state rather than to the triplet excited state.[27] The BET rate was determined from the disappearance of the absorption band at 790 nm due to $ZnCh^{\bullet+}$ in $ZnCh^{\bullet+}-C_{60}^{\bullet-}$ (Figure 2b). The decay of the absorption band obeys first-order kinetics (Figure 2c). The k_{BET} value is determined as 9.1×10^3 s^{-1}. Measured k_{BET} values for other linked porphyrin fullerene systems range from 1.6×10^{10} to 3.7×10^5 s^{-1},[1,22] and the value measured for $ZnCh^{\bullet+}-C_{60}^{\bullet-}$ thus corresponds to the longest lived radical ion pair ever reported for any D−A dyad system containing a porphyrin or chlorin as the donor and C_{60} as the acceptor.[1−9,21]

Formation of such a long-lived radical ion pair state of $ZnCh^{\bullet+}-C_{60}^{\bullet-}$ enabled detection of the radical ion species produced by PET with measurements of the ESR spectrum under photoirradiation of the compound. The resulting spectrum of the photoirradiated dyad **7** in PhCN at 143 K is shown in Figure 5a. The ESR spectrum consists of two characteristic signals, one of which is attributable to an organofullerene radical anion derivative at a small g value ($g = 2.0006$)[28], and the other to the chlorin radical cation at a higher g value ($g = 2.0031$). To confirm these assignments, the $ZnCh^{\bullet+}$ and $C_{60}^{\bullet-}$ spectra were produced independently via chemical oxidation of **7** with $Ru(bpy)_3^{3+}$ (bpy = 2,2′-bipyridine) and via chemical reduction with tetramethylsemiquinone radical anion as shown in Figure 5b,c, respectively. A comparison of the photochemically produced spectrum in Figure 5a with the spectrum of the chemically generated $ZnCh^{\bullet+}-C_{60}$ and $ZnCh-C_{60}^{\bullet-}$ in Figure 5b,c clearly shows that the observed ESR signal in Figure 5a is composed of two signals, one of which is due to the chlorin radical cation in Figure 5b, and the other due to $C_{60}^{\bullet-}$ in Figure 5c.

Upon "turning off" the irradiation source, no significant decay of the ESR signal occurred for hours. This indicates that PET from ^{1}ZnCh* to C_{60} results in formation of the radical ion pair ($ZnCh^{\bullet+}-C_{60}^{\bullet-}$) and that intermolecular electron transfer between radical ion pairs located close to each other in frozen PhCN occurs to give $ZnCh^{\bullet+}-C_{60}$ and $ZnCh-C_{60}^{\bullet-}$, which are now separated from each other to prevent the BET.

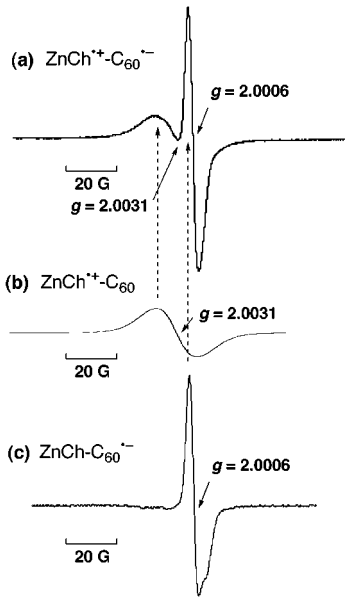

Figure 5. ESR spectra measured at 143 K of (a) the photoirradiated dyad ZnCh−C_{60} (**7**) (5.0×10^{-4} M) with a high-pressure mercury lamp, (b) oxidized **7** with $[Ru(bpy)_3](PF_6)_3$ (5.0×10^{-4} M), and (c) reduced **7** with tetramethyl-*p*-benzosemiquinone radical anion (5.0×10^{-4} M).

In contrast to the case of ZnCh−C_{60} (**7**), no transient formation of $C_{60}^{\bullet-}$ was detected at 1000 nm for any other dyad employed in this study (**6**, **9**, and **10**). In each case, only the triplet−triplet absorption due to the chlorin or porphyrin moiety was observed because of the higher energy of the radical ion pair as compared to the triplet excited state, as is expected from the redox potentials (vide supra). Because the fluorescence emission of **6** at $\lambda_{max} = 720$ nm is significantly quenched ($\Phi = 0.01$) as compared to the reference compound without the C_{60} moiety (**2**) at $\lambda_{max} = 720$ nm ($\Phi = 0.06$), the photoinduced electron transfer from ^1H_2Ch* to C_{60} may occur to give the radical ion pair ($H_2Ch^{\bullet+}-C_{60}^{\bullet-}$). The fluorescence lifetime of **2** ($\tau(\mathbf{2}) = 2.7$ ns) was significantly reduced when **2** is replaced by **6** ($\tau(\mathbf{6}) = 2.2 \times 10^2$ ps). The rate constant of electron transfer (k_{ET}) from ^1H_2Ch* to C_{60} is determined from the difference between $\tau(\mathbf{6})^{-1}$ and $\tau(\mathbf{2})^{-1}$ to be 4.2×10^9 s^{-1}. Similarly, the k_{ET} values of electron transfer from ^{1}ZnPor* and $^1H_2$Por* to C_{60} in **10** and **9** were determined to be 7.4×10^9 and 6.6×10^8 s^{-1}, respectively (Table 1).[29]

To quantify the driving force dependence on the ET rate constants (k_{ET}), eq 1 was employed, where V is the electronic coupling matrix element, k_B is the Boltzmann constant, h is the Planck constant, and T is the absolute temperature.[30] This

$$k_{ET} = \left(\frac{4\pi^3}{h^2\lambda k_B T}\right)^{1/2} V^2 \exp\left[-\frac{(\Delta G^\circ_{ET} + \lambda)^2}{4\lambda k_B T}\right] \qquad (1)$$

equation is rewritten as eq 2, which is also applied to evaluate

(24) The S_1 values of **7**, **10**, **6**, and **9** are obtained from the absorption maxima (see Experimental Section) and the emission maxima ($\lambda_{max} = 702$, 685, 720, and 682 nm) as 1.80, 1.84, 1.74, and 1.84 eV, respectively.

(25) Anderson, J. L.; An, Y.-Z.; Rubin, Y.; Foote, C. S. *J. Am. Chem. Soc.* **1994**, *116*, 9763.

(26) Dvornikov, S. S.; Knyukshto, V. N.; Solovev, K. N.; Tsvirko, M. P. *Opt. Spectrosk.* **1979**, *46*, 385.

(27) The energy level of the radical ion pair in reference to the triplet energy of a component is an important factor in determining the lifetime of the radical ion pair. See: (a) ref 22b. (b) Komamine, S.; Fujitsuka, M.; Ito, O.; Moriwaki, K.; Miyata, T.; Ohno, T. *J. Phys. Chem. A* **2000**, *104*, 1149. (c) Fujitsuka, M.; Ito, O.; Yamashiro, T.; Aso, Y.; Otsubo, T. *J. Phys. Chem. A* **2000**, *104*, 4876. (d) Fujitsuka, M.; Matsumoto, K.; Ito, O.; Yamashiro, Y.; Aso, Y.; Otsubo, T. *Res. Chem. Intermed.* **2000**, *27*, 73.

(28) For the g values of ESR spectra of C_{60} derivatives, see: Fukuzumi, S.; Mori, H.; Suenobu, T.; Imahori, H.; Gao, X.; Kadish, K. M. *J. Phys. Chem. A* **2000**, *104*, 10688.

(29) The fluorescence lifetimes of the reference porphyrin compounds are taken from ref 22a.

(30) (a) Marcus, R. A. *Annu. Rev. Phys. Chem.* **1964**, *15*, 155. (b) Marcus, R. A.; Sutin, N. *Biochim. Biophys. Acta* **1985**, *811*, 265. (c) Marcus, R. A. *Angew. Chem., Int. Ed. Engl.* **1993**, *32*, 1111.

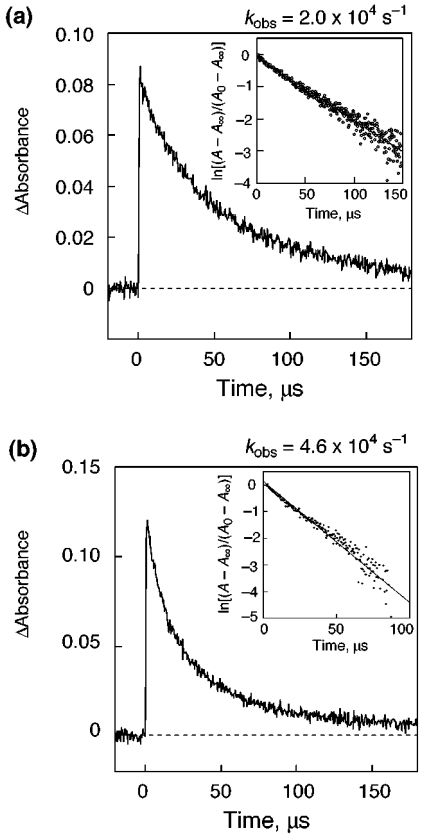

Figure 6. Kinetic traces for the triplet absorption at 500 nm for (a) **10** and (b) **9**. Inset: first-order plots.

the back electron transfer rate constant (k_{BET}). According to eq

$$k_B T \ln k_{ET} + \frac{\Delta G^\circ_{ET}}{2} = k_B T \ln\left[\left(\frac{4\pi^3}{h^2 \lambda k_B T}\right)^{1/2} V^2\right] - \frac{\lambda}{4} - \frac{(\Delta G^\circ_{ET})^2}{4\lambda} \quad (2)$$

2, a plot of $k_B T \ln k_{ET} + (\Delta G^\circ_{ET}/2)$ versus $(\Delta G^\circ_{ET})^2$ gives a linear correlation (see Supporting Information S3).[31] The λ and V values are obtained from the intercept and the slope as $\lambda = 0.484$ eV and $V = 6.79$ cm^{-1}, respectively. The k_{ET} and k_{BET} values are calculated from the λ, V, and ΔG°_{ET} (or ΔG°_{BET}) values using eq 1. The calculated k_{ET} and k_{BET} values are listed in Table 1 (see the values in parentheses), where the calculated values agree with the experimental values.[32]

The λ value (0.484 eV) in the present dyad systems is smaller than the value (0.66 eV) reported for zinc tetraphenylporphyrin−C_{60} dyad with an edge-to-edge distance (R_{ee}) of 11.9 Å.[22,33] The R_{ee} value between H_2Ch and C_{60} in the dyad (**6**) is evaluated as 5.89 Å from the optimized structure which was calculated by the PM3 method (see Experimental Section).[17] The smaller R_{ee} value in the present system may result in the smaller solvent reorganization energy as compared to the zinc tetraphenylporphyrin−C_{60} dyad system, because the smaller the R_{ee}, the smaller the solvent reorganization energy will be, as expected from the Marcus theory of electron transfer.[30,33] The solvent reorganization in ET of C_{60} and porphyrins is known to play a major role in determining the overall λ value, which includes a small reorganization energy of the inner coordination spheres associated with the little structural change in ET of C_{60} and porphyrins.[34,35] The smaller R_{ee} value also results in the larger V value (6.8 cm^{-1}) as compared to the value (3.9 cm^{-1}) of the zinc porphyrin−C_{60} system with a larger R_{ee} value.[33]

Scheme 2

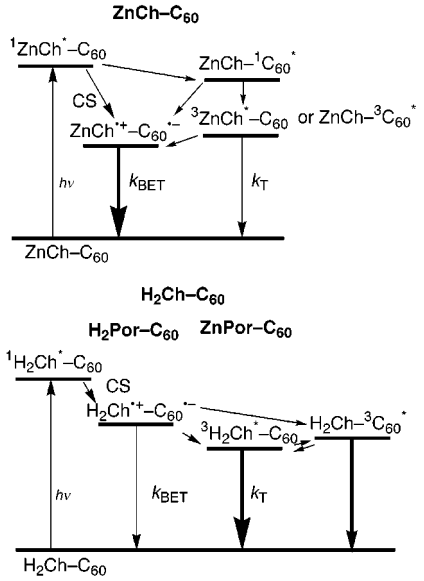

The photoinduced ET processes in the dyads in Table 1 are located in the normal region of the Marcus parabola ($\Delta G^\circ_{ET} > -\lambda$), whereas the BET process from $C_{60}^{\bullet-}$ to $ZnCh^{\bullet-}$ in **7** is in the inverted region ($\Delta G^\circ_{BET} < -\lambda$).[30,36] In the inverted region, the k_{BET} value decreases with the decreasing λ value.[30] Thus, the small λ value in the present dyad systems leads to the small k_{BET} value (9.1×10^3 s^{-1}) as compared to the value of any other D−A dyad system containing a porphyrin or chlorin as the donor and C_{60} as the acceptor.[1−9,22]

The radical ion pair derived from **6** cannot be detected in the microsecond time scale in Figure 2 because of the fast decay to the triplet excited state ($^3H_2Ch^*$−C_{60}) which is lower in energy than the radical ion pair.[27] The other dyads, **9** and **10**, also quickly yield the triplet excited states. The triplet decay rate constants (k_T) of **6**, **9**, and **10** and the reference compounds (**2** and **3**) were also determined (Figure 6), as listed in Table 1. The larger k_T values of **6**, **9**, and **10** as compared to the reference compounds (**2** and **3**) may be ascribed to the contribution of the decay from the triplet excited state of the C_{60} moiety, which is slightly higher in energy but has the shorter lifetime.[22]

(31) The correlation coefficient (ρ) of a least-squares linear fit was $\rho = 1.000$ (S3).

(32) The agreement between the calculated k_{BET} value and the experimental value is quite sensitive to the λ and V values. For example, slightly different values (2% larger values: $\lambda = 0.494$ eV and $V = 6.93$ cm^{-1}) give the calculated k_{BET} value (1.8×10^4 s^{-1}) which is twice as large as the experimental value (9.1×10^3 s^{-1}). Thus, uncertainty in the λ and V values may be within ±2%.

(33) (a) Imahori, H.; Tamaki, K.; Guldi, D. M.; Luo, C.; Fujitsuka, M.; Ito, O.; Sakata, Y.; Fukuzumi, S. *J. Am. Chem. Soc.* **2001**, *123*, 2607. (b) Imahori, H.; Guldi, D. M.; Tamaki, K.; Yoshida, Y.; Luo, C.; Sakata, Y.; Fukuzumi, S. *J. Am. Chem. Soc.* **2001**, *123*, 6617. (c) Imahori, H.; Tkachenko, N. V.; Vehmanen, V.; Tamaki, K.; Lemmetyinen, H.; Sakata, Y.; Fukuzumi, S. *J. Phys. Chem. A* **2001**, *105*, 1750.

(34) Fukuzumi, S.; Nakanishi, I.; Suenobu, T.; Kadish, K. M. *J. Am. Chem. Soc.* **1999**, *121*, 3468.

(35) Fukuzumi, S.; Nakanishi, I.; Tanaka, K.; Suenobu, T.; Tabard, A.; Guilard, R.; Van Caemelbecke, E.; Kadish, K. M. *J. Am. Chem. Soc.* **1999**, *121*, 785.

(36) For the Marcus inverted region, see: (a) Closs, G. L.; Miller, J. R. *Science* **1988**, *240*, 440. (b) Gould, I. R.; Farid, S. *Acc. Chem. Res.* **1996**, *29*, 522. (c) McLendon, G. *Acc. Chem. Res.* **1988**, *21*, 160. (d) Winkler, J. R.; Gray, H. B. *Chem. Rev.* **1992**, *92*, 369. (e) McLendon, G.; Hake, R. *Chem. Rev.* **1992**, *92*, 481. (f) Mataga, N.; Miyasaka, H., In *Electron Transfer from Isolated Molecules to Biomolecules Part 2*; Jortner, J., Bixon, M., Eds.; Wiley: New York, 1999; p 431.

In conclusion, the ZnCh−C_{60} dyad (**7**) gives a long-lived radical ion pair upon photoexcitation, whereas photoexcitation of the other dyads having the same linkage (H_2Ch−C_{60}, ZnPor−C_{60}, and H_2Por−C_{60}) gives short-lived radical ion pairs which decay to give the triplet excited states, because the radical ion pair is higher in energy, as schematically shown in Scheme 2. This demonstrates the importance of the zinc chlorin chloromophore instead of a fully conjugated porphyrin system to obtain the long-lived charge separated state.

Acknowledgment. This work was partially supported by a Grant-in-Aid for Scientific Research Priority Area (No. 11228205) from the Ministry of Education, Science, Culture and Sports, Japan and the Robert A. Welch Foundation (K.M.K., Grant E−680). Our special thanks are due to Dr. Suresh Das, Regional Research Laboratory, Trivendrum, India for the fluorescence measurements.

Supporting Information Available: Synthesis of **2** and **3** (S1), transient absorption spectrum of **7** between 400 and 800 nm (S2), and plot of $RT \ln k_{ET} + \Delta G°_{ET}$ vs $(\Delta G°_{ET})^2$ (S3). This material is available free of charge via the Internet at http://pubs.acs.org.

JA015738A